Journal of Organometallic Chemistry, 252 (1983) 243–255
Elsevier Sequoia S.A., Lausanne – Printed in The Netherlands

CLUSTER CHEMISTRY

XXIII *. MONO-, DI- AND TRI-AURATION OF $H_4Ru_4(CO)_{12}$ WITH $[\{Au(PPh_3)\}_3O][BF_4]$: X-RAY CRYSTAL STRUCTURE OF $HRu_4Au_3(CO)_{12}(PPh_3)_3$

MICHAEL I. BRUCE* and BRIAN K. NICHOLSON **

Jordan Laboratories, Department of Physical and Inorganic Chemistry, University of Adelaide, South Australia, 5001 (Australia)

(Received February 28th, 1983)

Summary

Reactions between $[H_3Ru_4(CO)_{12}]^-$ and $[\{Au(PPh_3)\}_3O]^+$ afford $H_3Ru_4Au(CO)_{12}(PPh_3)$, $H_2Ru_4Au_2(CO)_{12}(PPh_3)_2$ and $HRu_4Au_3(CO)_{12}(PPh_3)_3$. The X-ray structure of the latter shows that it has the unusual bicapped trigonal bipyramidal metal core, in which two Ru_2Au faces of the Ru_4Au fragment are capped by the other two Au atoms. The central Au atom is asymmetrically attached to the Ru_3 face as a result of the interaction of a phenyl ring of the PPh_3 ligand with two of the CO groups. Metal–metal separations are: two Au–Au, 2.837(1) Å; Ru–Ru, six between 2.805–3.004(3) Å; Au–Ru, seven between 2.821–3.007(2) Å. $HRu_4Au_3(CO)_{12}(PPh_3)_3$ is monoclinic, space group $P2_1/n$, with a 18.754(3), b 18.459(5), c 22.317(4) Å, β 113.06(2)°; 2852 data [$I > 2.5\sigma(I)$] were refined to R, R_w 0.038, 0.038.

Introduction

Over the last two years, the number of heteronuclear metal clusters incorporating gold atoms in the metal core has increased rapidly [1–13]. Among these, several gold-ruthenium and gold-osmium clusters have been characterised by X-ray structural studies, including $HOs_4Au(CO)_{13}(PEt_3)$ [3], $H_3Os_4Au(CO)_{12}(PEt_3)$ [3], $H_2Os_4Au_2(CO)_{12}(PPh_3)_2$ [4], $RuCo_3Au(CO)_{12}(PPh_3)$ [6], $HOs_3Au(CO)_{10}(PPh_3)$ [7], $Os_3Au(\mu\text{-SCN})(CO)_{10}(PPh_3)$ [7], $HRu_3Au(\mu_3\text{-PPh})(CO)_9(PMe_2Ph)$ [8], $[H_2Os_6Au(CO)_{20}]^-$ [9], $H_2Ru_3Au[\mu_3\text{-C(OMe)}](CO)_9(PPh_3)$ [10], $Ru_3Au_3[\mu_3\text{-C(OMe)}](CO)_9(PPh_3)_3$ [10], $Ru_3CoAu_3(CO)_{12}(PPh_3)_3$ [11] and $Ru_3Au(\mu_3\text{-}C_2Bu^t)(CO)_9(PPh_3)$ [12]. That the majority of these contain only one or two gold atoms per molecule is a result of their isolation from reactions between cluster anions and $AuCl(PR_3)$ (the presence of $TlPF_6$ often facilitates the reaction by

* For Part XXII, see ref. 30.

** On leave from the University of Waikato, Hamilton (New Zealand).

0022-328X/83/$03.00

removing chloride) or $[Au(PR_3)]^+$. Few cluster anion precursors with three or more negative charges are known, although three gold moieties can be added to the anions $[M(CO)_4]^{3-}$ (M = Mn or Re) [13] and $[V(CO)_5]^{3-}$ [14]; the latter complex has a tetrahedral Au_3V core. Recently, the Bristol group has prepared several trigold-metal clusters from reactions between $AuMe(PPh_3)$ and cluster hydride precursors, which proceed by elimination of CH_4 [10].

We have described briefly the application of the gold-oxonium reagent $[\{Au(PPh_3)\}_3O][BF_4]$ to the syntheses of poly-gold mixed metal clusters [11]. Herein are given details of reactions of this reagent with Ru_4 clusters to give derivatives containing one, two and three gold atoms, together with a description of the structure of $HAu_3Ru_4(CO)_{12}(PPh_3)_3$. A brief report on the structure of this complex appeared during the course of this study [10].

Experimental

Reactions were routinely performed in Schlenk equipment under an atmosphere of dry nitrogen, although this was probably only necessary for reactions involving $[H_3Ru_4(CO)_{12}]^-$; other reactants and products were apparently not air-sensitive. Tetrahydrofuran (THF) was freshly distilled from sodium diphenylketyl, while other hydrocarbon solvents were dried over sodium wire. Petroleum spirit refers to a fraction of b.p. 40–60°C. The compounds $H_4Ru_4(CO)_{12}$ [15] and $[\{Au(PPh_3)\}_3O][BF_4]$ [16] were prepared by the literature methods; K-Selectride ($K[HB(CHMeEt)_3]$) was used as a 0.5 mol l^{-1} solution in THF, as received from Aldrich Chemicals.

Reaction between $[H_3Ru(CO)_{12}]^-$ and $[\{Au(PPh_3)\}_3O][BF_4]$

A solution of $[H_4Ru_4(CO)_{12}]$ (0.10 g, 0.135 mmol) in THF (7 cm^3) was treated with K-Selectride (0.30 cm^3 of a 0.5 mol l^{-1} solution in THF) for 15 min. An infrared spectrum of an aliquot extracted from the reaction mixture showed complete conversion to $[H_3Ru_4(CO)_{12}]^-$ [ν(CO) (THF) 2040m, 2020m, 2000s cm^{-1}] [17]. Solid $[\{Au(PPh_3)\}_3O][BF_4]$ (0.18 g, 0.12 mmol) was added and the mixture stirred for 4 h. After removal of the solvent the residue was chromatographed on silica gel plates, eluting with benzene/petroleum spirit (1/1). Four bands developed:

Band 1: red-orange, $R_f = 0.95$, was recrystallised from Et_2O/petroleum spirit (1/2) to give deep red crystals, identified as $[H_3Ru_4Au(CO)_{12}(PPh_3)]$ (I) (15 mg, 10%). Found: C, 29.99; H, 1.54. $C_{30}H_{18}AuO_{12}PRu_4$ calcd.: C, 29.96; H, 1.51%. IR: ν(CO) (hexane) 2092s, 2084w, 2066vs, 2052s, 2039sh, 2032vs, 2015m, 2003sh, 1982m, 1979m, 1960m, 1900w cm^{-1}; ^1H NMR δ ($CDCl_3$) 7.45, m, Ph; −17.7, s, Ru *H*.

Band 2: red-orange, $R_f = 0.90$, traces, IR ν(CO) (hexane) 2092w, 2078s, 2065m, 2044s, 2031vs, 2012vs, 1971s, 1948w(sh), 1898w cm^{-1}, not further investigated.

Band 3: brown, $R_f = 0.60$, recrystallised from CH_2Cl_2/petroleum spirit (1/2) to give red-brown needles, identified as $[H_2Ru_4Au_2(CO)_{12}(PPh_3)_2]$ (II), (6 mg, 3%). Found: C, 35.88; H, 1.90. $C_{48}H_{32}Au_2O_{12}P_2Ru_4$ calcd.: C, 34.71; H, 1.94%. IR: ν(CO) [CH_2Cl_2/hexane (1/1)] 2092w, 2074s, 2047s, 2036s, 2027vs, 2011s, 1995m, 1981m, 1960m, 1925w, 1900w cm^{-1}. (cf. $H_2Au_2Os_4(CO)_{12}(PPh_3)_2$ (isomer A): ν(CO) 2077s, 2055(sh), 2050s, 2026s, 2013m, 1999m, 1991m, 1941w(br), 1903w(br) cm^{-1} [4]).

Band 4: green, $R_f = 0.35$, recrystallised from CH_2Cl_2/petroleum spirit as very

fine needles with a bronze sheen (43 mg, 15%) identified as $[HRu_4Au_3(CO)_{12}(PPh_3)_3]$ (III). Found: C, 37.22; H, 2.09. $C_{66}H_{46}Au_3O_{12}P_3Ru_4$ calcd.: C, 37.41, H, 2.19%. IR: ν(CO) (CH_2Cl_2) 2092w, 2056vs, 2016(sh), 2010vs, 1992s, 1970m, 1956m, 1924w cm^{-1}. ^1H NMR δ ($CDCl_3$) 1.72, m, Ph; −13.3, m, Ru–*H*. λ_{max} ($CHCl_3$) 425 nm; λ_{max} (benzene) 425 nm, 630 nm.

Crystal structure of $[HRu_4Au_3(CO)_{12}(PPh_3)_3]$ (III)

A single intensely coloured, brown-red crystal of dimension $0.11 \times 0.10 \times 0.08$ mm was finally obtained by slow diffusion of Et_2O into a concentrated CH_2Cl_2 solution. Lattice parameters were derived from a least-squares fit to the setting angles of 25 high angle reflections on an Enraf-Nonius CAD-4 diffractometer with graphite monochromated Mo-K_α radiation.

(Continued on p. 249)

TABLE 1

FINAL POSITIONAL PARAMETERS FOR $Au_3Ru_4(H)(CO)_{12}(PPh_3)_3$

Atom	*x*	*y*	*z*
Au(1)	350(1)	2519(1)	8120(1)
Au(2)	261(1)	2780(1)	6841(1)
Au(3)	−1001(1)	1929(1)	8213(1)
Ru(1)	959(1)	1467(1)	7429(1)
Ru(2)	165(1)	916(1)	8255(1)
Ru(3)	4260(1)	3251(1)	2053(1)
Ru(4)	4861(1)	4652(1)	2010(1)
P(1)	830(3)	3444(3)	8851(3)
P(2)	266(3)	3734(3)	6182(3)
P(3)	−1945(3)	2051(3)	8621(3)
C(11)	1604(14)	659(13)	7645(12)
C(12)	1786(15)	2143(15)	7735(14)
C(13)	940(15)	1531(15)	6572(15)
C(21)	795(16)	159(16)	8567(15)
C(22)	−690(15)	319(14)	8154(14)
C(23)	354(12)	1250(12)	9095(12)
C(31)	−984(13)	1619(13)	6171(14)
C(32)	−1655(14)	1310(13)	6960(13)
C(33)	−1128(12)	2709(12)	6986(11)
C(41)	422(14)	−482(15)	7272(13)
C(42)	−1063(16)	−123(14)	6779(14)
C(43)	−178(17)	279(17)	6196(17)
O(11)	2073(9)	201(9)	7866(9)
O(12)	2344(11)	2505(10)	7967(9)
O(13)	956(12)	1491(11)	6066(11)
O(21)	1184(11)	−372(11)	8831(10)
O(22)	−1201(11)	−26(10)	8169(10)
O(23)	514(10)	1341(9)	9664(10)
O(31)	−1126(10)	1552(10)	5607(10)
O(32)	−2293(10)	1072(9)	6827(9)
O(33)	−1427(8)	3268(8)	6920(7)
O(41)	741(10)	−1036(11)	7430(10)
O(42)	−1654(12)	−428(11)	6587(10)
O(43)	4886(12)	4849(12)	700(12)
C(111)	1620(8)	3963(8)	8803(10)

(continued)

TABLE 1 (continued)

Atom	*x*	*y*	*z*
C(112)	2215(8)	4244(8)	9353(10)
C(113)	2805(8)	4651(8)	9285(10)
C(114)	2801(8)	4778(8)	8667(10)
C(115)	2206(8)	4497(8)	8118(10)
C(116)	1615(8)	4090(8)	8186(10)
C(121)	1247(8)	3079(8)	9678(6)
C(122)	955(8)	3208(8)	10155(6)
C(123)	1295(8)	2874(8)	10763(6)
C(124)	1926(8)	2411(8)	10893(6)
C(125)	2218(8)	2282(8)	10416(6)
C(126)	1879(8)	2616(8)	9809(6)
C(131)	128(8)	4110(8)	8860(8)
C(132)	−647(8)	3900(8)	8641(8)
C(133)	−1209(8)	4397(8)	8638(8)
C(134)	−996(8)	5104(8)	8854(8)
C(135)	−220(8)	5315(8)	9073(8)
C(136)	341(8)	4818(8)	9076(8)
C(141)	1059(8)	3667(8)	5896(9)
C(142)	1796(8)	3510(8)	6360(9)
C(143)	2418(8)	3431(8)	6172(9)
C(144)	2304(8)	3509(8)	5519(9)
C(145)	1567(8)	3666(8)	5054(9)
C(146)	944(8)	3745(8)	5243(9)
C(151)	−614(7)	3734(9)	5447(6)
C(152)	−810(7)	3101(9)	5077(6)
C(153)	−1488(7)	3072(9)	4514(6)
C(154)	−1971(7)	3678(9)	4321(6)
C(155)	−1775(7)	4311(9)	4691(6)
C(156)	−1097(7)	4340(9)	5254(6)
C(161)	325(9)	4621(7)	6516(8)
C(162)	−43(9)	4741(7)	6943(8)
C(163)	4(9)	5419(7)	7232(8)
C(164)	418(9)	5977(7)	7094(8)
C(165)	785(9)	5857(7)	6667(8)
C(166)	739(9)	5179(7)	6378(8)
C(171)	−2246(9)	1139(6)	8742(9)
C(172)	−1915(9)	801(6)	9348(9)
C(173)	−2076(9)	75(6)	9415(9)
C(174)	−2569(9)	−314(6)	8875(9)
C(175)	−2900(9)	23(6)	8269(9)
C(176)	−2739(9)	750(6)	8202(9)
C(181)	−2838(8)	2479(9)	8057(8)
C(182)	−2784(8)	2981(9)	7610(8)
C(183)	−3448(8)	3335(9)	7187(8)
C(184)	−4166(8)	3186(9)	7211(8)
C(185)	−4220(8)	2684(9)	7658(8)
C(186)	−3556(8)	2331(9)	8081(8)
C(191)	−1703(11)	2531(10)	9383(7)
C(192)	−2233(11)	3002(10)	9476(7)
C(193)	−2048(11)	3343(10)	10075(7)
C(194)	−1333(11)	3215(10)	10582(7)
C(195)	−803(11)	2744(10)	10490(7)
C(196)	−988(11)	2403(10)	9890(7)

TABLE 2

BOND LENGTHS FOR $HRu_4Au_3(CO)_{12}(PPh_3)_3$ (Å)

Au(2)–Au(1)	2.835(2)	C(31)–Ru(3)	1.854(25)
Au(3)–Au(1)	2.838(1)	C(32)–Ru(3)	1.834(27)
Ru(1)–Au(1)	2.972(2)	C(33)–Ru(3)	1.899(27)
Ru(2)–Au(1)	3.008(2)	C(41)–Ru(4)	1.820(29)
Ru(3)–Au(1)	2.838(2)	C(42)–Ru(4)	1.823(26)
P(1)–Au(1)	2.288(6)	C(43)–Ru(4)	1.794(28)
Ru(1)–Au(2)	2.822(2)	C(11)–O(11)	1.179(29)
Ru(3)–Au(2)	2.840(2)	C(12)–O(12)	1.177(32)
P(2)–Au(2)	2.297(6)	C(13)–O(13)	1.144(45)
Ru(2)–Au(3)	2.849(2)	C(21)–O(21)	1.224(34)
Ru(3)–Au(3)	2.837(2)	C(22)–O(22)	1.162(37)
P(3)–Au(3)	2.297(8)	C(23)–O(23)	1.197(34)
Ru(2)–Ru(1)	2.968(3)	C(31)–O(31)	1.187(37)
Ru(3)–Ru(1)	3.005(3)	C(32)–O(32)	1.197(32)
Ru(4)–Ru(1)	2.805(3)	C(33)–O(33)	1.156(27)
C(11)–Ru(1)	1.861(24)	C(41)–O(41)	1.167(33)
C(12)–Ru(1)	1.897(27)	C(42)–O(42)	1.165(34)
C(13)–Ru(1)	1.903(25)	C(43)–O(43)	1.183(30)
Ru(3)–Ru(2)	2.980(3)	P(1)–C(111)	1.801(18)
Ru(4)–Ru(2)	2.814(3)	P(1)–C(121)	1.830(14)
C(21)–Ru(2)	1.785(29)	P(1)–C(131)	1.807(17)
C(22)–Ru(2)	1.884(29)	P(2)–C(141)	1.836(21)
C(23)–Ru(2)	1.869(27)	P(2)–C(151)	1.814(12)
Ru(4)–Ru(3)	2.837(3)	P(2)–C(161)	1.784(16)
		P(3)–C(171)	1.829(15)
		P(3)–C(181)	1.832(15)
		P(3)–C(191)	1.811(18)

TABLE 3

SELECTED BOND ANGLES FOR $HRu_4Au_3(CO)_{12}(PPh_3)_3$ (°) [a]

Au(3)–Au(1)–Au(2)	115.9(1)	Au(3)–Ru(3)–Au(2)	115.8(1)
Ru(1)–Au(1)–Au(3)	108.8(1)	Ru(1)–Ru(3)–Au(2)	57.7(1)
Ru(2)–Au(1)–Au(2)	107.8(1)	Ru(1)–Ru(3)–Au(3)	108.0(1)
P(1)–Au(1)–Au(2)	116.3(2)	Ru(2)–Ru(3)–Au(2)	108.4(1)
P(1)–Au(1)–Au(3)	110.3(2)	Ru(4)–Ru(3)–Au(1)	108.7(1)
Ru(1)–Au(2)–Au(1)	63.4(1)	Ru(4)–Ru(3)–Au(2)	107.9(1)
Ru(3)–Au(2)–Ru(1)	64.1(1)	Ru(4)–Ru(3)–Au(3)	110.5(1)
P(2)–Au(2)–Au(1)	139.6(2)	Ru(4)–Ru(3)–Ru(1)	57.3(1)
Ru(2)–Au(3)–Au(1)	63.9(1)	Ru(4)–Ru(3)–Ru(2)	57.8(1)
Ru(3)–Au(3)–Ru(2)	63.2(1)	C(32)–Ru(3)–C(31)	89.5(15)
P(3)–Au(3)–Au(1)	147.1(2)	C(33)–Ru(3)–C(31)	96.3(13)
Ru(2)–Ru(1)–Au(2)	109.2(1)	C(33)–Ru(3)–C(32)	95.2(13)
Ru(3)–Ru(1)–Au(1)	56.7(1)	C(42)–Ru(4)–C(41)	93.2(13)
Ru(4)–Ru(1)–Au(1)	105.8(1)	C(43)–Ru(4)–C(41)	93.1(14)
Ru(4)–Ru(1)–Au(2)	109.3(1)	C(43)–Ru(4)–C(42)	91.3(14)
C(12)–Ru(1)–C(11)	94.4(11)	C(111)–P(1)–Au(1)	117.3(7)
C(13)–Ru(1)–C(11)	93.7(12)	C(121)–P(1)–Au(1)	109.8(5)
C(13)–Ru(1)–C(12)	90.7(13)	C(131)–P(1)–Au(1)	115.5(5)
Ru(1)–Ru(2)–Au(3)	108.6(1)	C(141)–P(2)–Au(2)	112.2(6)
Ru(3)–Ru(2)–Au(1)	56.6(1)	C(151)–P(2)–Au(2)	110.4(6)
Ru(4)–Ru(2)–Au(1)	104.7(1)	C(161)–P(2)–Au(2)	116.8(7)
Ru(4)–Ru(2)–Au(3)	110.8(1)	C(171)–P(3)–Au(3)	107.4(7)
C(22)–Ru(2)–C(21)	89.5(13)	C(181)–P(3)–Au(3)	114.2(7)
C(23)–Ru(2)–C(21)	91.8(13)	C(191)–P(3)–Au(3)	118.2(7)
C(23)–Ru(2)–C(22)	97.6(12)		

[a] All other M–M–M angles are 60 ± 2°; Ru–C–O angles are between 169 and 178°.

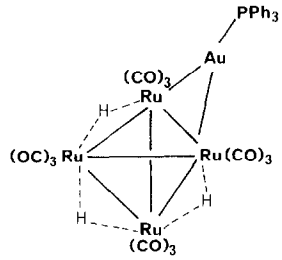

I

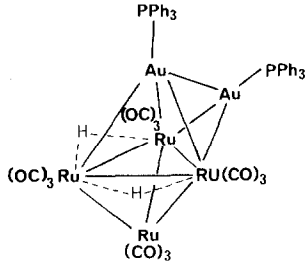

II

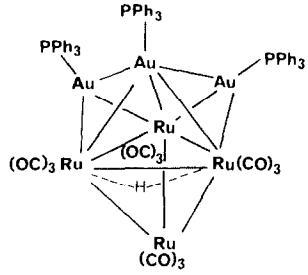

III

Crystal data

$C_{66}H_{46}Au_3O_{12}P_3Ru_4$, $M_r = 2119.2$, Monoclinic, space group $P2_1/n$ * (a non-standard setting of $P2_1/c$), a 18.754(3), b 18.459(5), c 22.317(4) Å, β 113.06(2)°, U 7108.5 Å^3, D_m 1.96(2) g cm^{-3}, D_c 1.980 g cm^{-3} for $Z = 4$, $F(000) = 3984$, μ(Mo-K_α) 71.6 cm^{-1}. Intensity data were collected in the range $1.5° < \theta < 18°$ using an $[\omega - n/3\theta]$ scan, where n was assigned a value of 2 based on peak shape analysis. Horizontal counter apertures and ω scan angles of $(2.40 + 0.35 \tan \theta)$ mm and $(0.80 + 0.35 \tan \theta)°$ were used. The data were corrected for Lorentz and polarisation effects (SUSCAD) [18] and for absorption (ABSORB) [19]. Of the 4186 unique reflections collected, those 2852 with $I > 2.5\ \sigma(I)$ were used in the refinement.

Structure solution and refinement

The positions of the three gold atoms were derived by direct methods (SHELX) [20] and subsequent refinement/difference fourier cycles revealed all other non-hydrogen atoms. In the final cycles of blocked full-matrix least-squares refinement the metal and phosphorus atoms were given anisotropic temperature factors, while other

* Equivalent positions $\pm (x, y, z;\ 1/2 - x,\ 1/2 + y,\ 1/2 - z)$.

atoms were treated isotropically. Phenyl rings were included as rigid groups (d_{C-C} 1.395 Å) but H atoms were not used in the model. Refinement converged with $R = 0.038$, $R_w = 0.038$ with a weighting scheme which converged to $w = 1.23\,[\sigma^2(F_o) + 0.0002\,F_o^2]^{-1}$. No parameter shifted by more than 0.1σ in the final cycle of refinement and a final difference map showed no peaks greater than 0.5 e $Å^{-3}$. Table 1 contains final positional parameters for the non-hydrogen atoms, while Tables 2 and 3 list bond lengths and selected bond angles for the cluster.

Results and discussion

The reaction between $[\{Au(PPh_3)\}_3O][BF_4]$ and $[H_3Ru_4(CO)_{12}]^-$ gives a mixture of clusters, $[H_{4-n}\{Au(PPh_3)\}_nRu_4(CO)_{12}]$ ($n = 1$–3) in which, formally, the equivalent number of hydride ligands of $H_4Ru_{14}(CO)_{12}$ have been replaced by 1–3 $Au(PPh_3)$ groups. This parallels observations previously reported for a number of mono-gold mixed-metal cluster systems where $Au(PPh_3)$ groups formally replace the H ligand of the corresponding hydride. However, the present examples are more complicated. Firstly monitoring the reaction by TLC and IR spectroscopy showed an initial rapid reaction occurred to give appreciable amounts of the mono-gold derivative (I). This was followed by a slower change over several hours in which increasing amounts of the tri-gold cluster (III) were formed at the expense of the mono-gold complex. A certain amount of the intermediate di-gold system (II) is found quite early in the reaction but this always remains a minor component. The use of a deficit of the oxonium reagent (ratio of $[H_3Ru_4(CO)_{12}]^-$ to $[\{Au(PPh_3)\}_3O]^+$ 2/1) did not alter this overall pattern although total yields were lowered. Therefore, a simple stepwise construction of the clusters by successive replacement of H ligands by $Au(PR_3)$ is apparently not occurring.

The gold-oxonium reagent is a strong aurating species; no clear reaction occurred between $[H_3Ru_4(CO)_{12}]^-$ and $AuCl(PPh_3)$ in THF. Use of the cluster anion was also necessary since a mixture of the neutral hydride $H_4Ru_4(CO)_{12}$ and the oxonium reagent in THF reacted very slowly and gave no clearly identifiable products. At this stage we are unable to explain the reaction mechanism. A number of other systems are being examined to establish patterns of reactivity for the oxonium reagent.

The bright orange mono-gold cluster $H_3AuRu_4(CO)_{12}(PPh_3)$ (I) was identified by normal techniques, and by comparison with some related species, differing only in the phosphine groups, which have been reported briefly [3]. We assume structure I for this cluster on the basis of the reported structure of the osmium analogue [3] $H_3Os_4Au(CO)_{12}(PPh_3)$, in which the $Au(PPh_3)$ group edge-bridges one Os–Os bond of the Os_4 tetrahedron. Similarly, the brown di-gold species $[H_2Au_2Ru_4(CO)_{12}(PPh_3)_2]$ was assigned structure II by comparison with the structurally characterised osmium analogue [4].

The tri-substituted cluster, $HRu_4Au_3(CO)_{12}(PPh_3)_3$ (III), forms red-black air-stable crystals which give brown solutions in hexane but intense green solutions in aromatic solvents; this can be traced to a broad, charge-transfer band at 630 nm for III in benzene which is absent in CH_2Cl_2. The molecular formula was indicated by analysis, and the presence of the hydride ligand shown by a single resonance at δ −13.3 in the ^1H NMR spectrum; a full X-ray crystal structure analysis was performed to determine the details of the metal arrangement.

Structure of $HRu_4Au_3(CO)_{12}(PPh_3)_3$ (III)

A general view of the molecule is given in Fig. 1, while details of the metal core geometry are shown in Fig. 2. A stereoview is given in Fig. 3. The complex consists of a tetrahedron of Ru atoms capped on one face by an Au atom with the remaining Au atoms capping two adjacent $AuRu_2$ faces. This gives overall a bicapped trigonal-bipyramidal (or tricapped tetrahedral) core. Each Au atom is bonded to a PPh_3 ligand, while each Ru carries three terminal CO groups. The detailed results of this study discussed below agree with those reported earlier within the latter's quoted errors [10], but are more accurate.

Although the H ligand was not directly located, the disposition of the carbonyl groups indicate that it bridges the Ru(1)–Ru(2) bond. The H atom must lie on the pseudo-mirror plane through Au(1)–Ru(3)–Ru(4) which relates to CO ligands; the regular arrangement of axial CO's on the Ru(1)–Ru(2)–Ru(4) face rule out a μ_3 location on this face. Considering the Ru(1)–Ru(2) and Ru(3)–Ru(4) edges, CO(12) and CO(23) form angles of 122.7 and 124.5°, respectively, with the former, suggesting that the μ_2-H ligand is almost capping the Au(1)–Ru(2)–Ru(1) face. The longer Ru(1)–Ru(2) separation [2.968(3) Å] is also consistent with the H atom bridging this bond.

It is immediately obvious that the analogy between H and $Au(PR_3)$, which arises out of the isolobal relationship between these two species [2], cannot be extended to the poly-gold complex III. The structure of $H_4Ru_4(CO)_{12}$ is based on a tetrahedral Ru_4 core, and the H atoms bridge four of the six Ru–Ru vectors resulting in D_{2d}

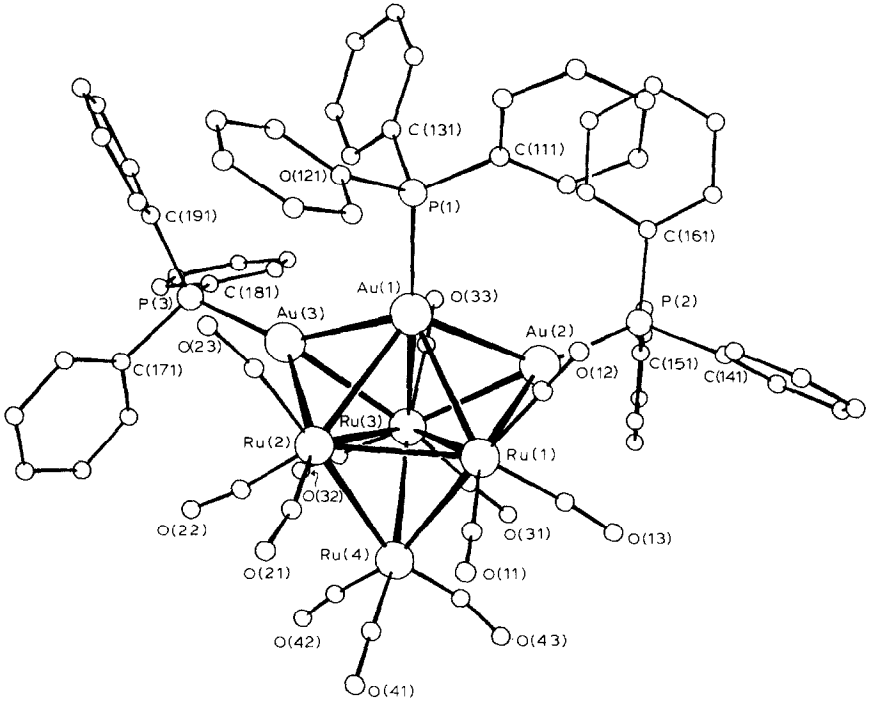

Fig. 1. A perspective view of a molecule of $HRu_4Au_3(CO)_{12}(PPh_3)_3$ (III) showing atom labelling scheme.

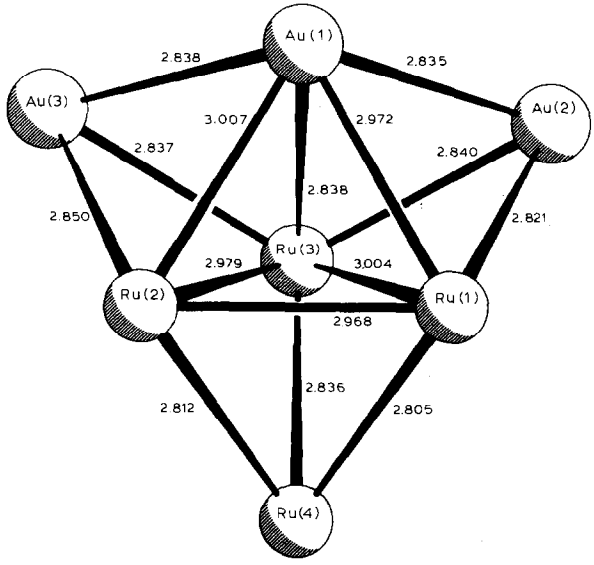

Fig. 2. A view of the metallic core of $HRu_4Au_3(CO)_{12}(PPh_3)_3$ (III) giving individual metal–metal bond distances. Standard deviations are 0.001, 0.002, 0.003 Å for Au–Au, Au–Ru and Ru–Ru bonds, respectively.

symmetry for the H_4Ru_4 moiety [21]. In contrast, while two of the $Au(PPh_3)$ groups could be considered to bridge the Ru(1)–Ru(3) and Ru(2)–Ru(3) edges, respectively, the Au–P vectors do not intersect these edges, and further, the third $Au(PPh_3)$ moiety not only caps the Ru(1)–Ru(2)–Ru(3) face, but is also within bonding distance of the other two gold atoms. The structure is related to that of $H_2Os_4Au_2(CO)_{12}(PPh_3)_2$ [4], in which the two gold atoms are within bonding distance of each other; one caps an Os_3 face, while the second caps one of the Os–Au faces so formed. Although in this instance, the Au(2)–Os(3) separation [3.159(4) Å] was considered to be outside the normal bonding distance, we believe

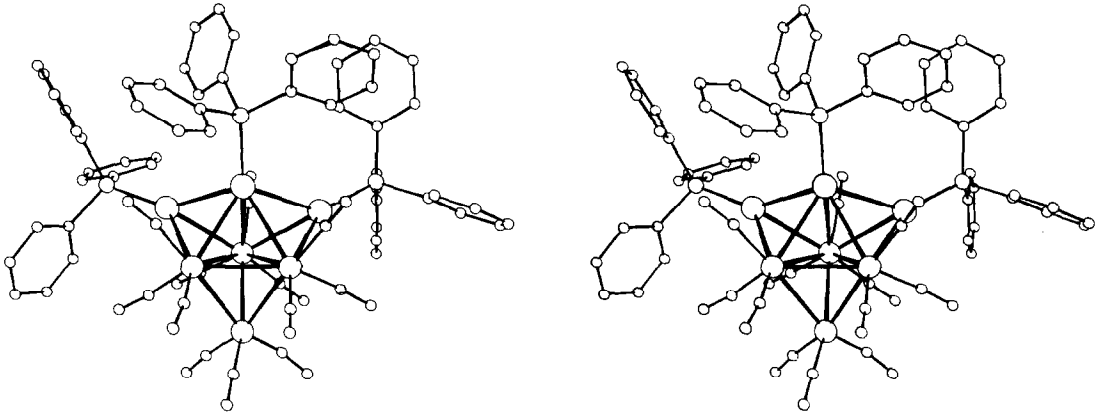

Fig. 3. A stereoview of $HRu_4Au_3(CO)_{12}(PPh_3)_3$ (III).

TABLE 4

COMPARISON OF CORE GEOMETRIES IN Ru_4Au_3, Ru_3Au_3 AND Ru_3CoAu_3 CLUSTERS

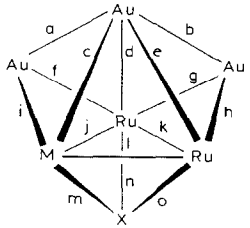

		Metal–metal separations (Å)			
	Complex	$HRu_4Au_3(CO)_{12}(PPh_3)_3$ [a]	$HRu_4Au_3(CO)_{12}(PPh_3)_3$ [b]	$Ru_3CoAu_3(CO)_{12}(PPh_3)_3$ [c]	$Ru_3Au_3[\mu_3\text{-}C(OMe)](CO)_9(PPh_3)_3$ [d]
	M	Ru	Ru	Co	Ru
	X	Ru	Ru	Ru	C
Au–Au	a	2.838(1)	2.819(4)	2.836(1)	3.010(1)
	b	2.835(1)	2.842(3)	2.784(1)	2.930(1)
Au–Ru	c	3.007(2)	2.956(6)	–	2.818(2)
	d	2.838(2)	2.839(5)	2.850(2)	2.987(2)
	e	2.972(2)	3.012(4)	3.054(3)	2.825(2)
	f	2.837(2)	2.838(5)	2.813(2)	2.844(2)
	g	2.840(2)	2.844(7)	2.783(2)	2.833(2)
	h	2.821(2)	2.843(4)	2.917(3)	2.796(2)
	i	2.850(2)	2.825(4)	–	2.807(2)
Au–Co	i	–	–	2.712(4)	–
Ru–Ru	j	2.979(3)	3.001(5)	–	2.913(2)
	k	3.004(3)	2.979(6)	2.992(3)	2.929(2)
	l	2.968(3)	2.962(8)	–	2.895(3)
	m	2.812(3)	2.803(5)	–	–
	n	2.836(3)	2.815(6)	2.869(4)	–
	o	2.805(3)	2.802(8)	2.844(2)	–
Ru–Co	j	–	–	2.825(4)	–
	l	–	–	2.710(3)	–
	m	–	–	2.692(4)	–

[a] This work. [b] Ref. [10]. [c] Ref. [11]. [d] Ref. [10].

that a weak interaction may exist between these atoms, with the metal core meriting the description of a capped trigonal-bipyramid. At the same time we note that the structure of $H_3Os_4Au(CO)_{12}(PEt_3)$ [3] is fully in accord with the suggestion that one of the H atoms in the $H_4Os_4(CO)_{12}$ parent has been replaced by an $Au(PEt_3)$ group.

The metal core geometry of III contains an interesting pattern of bond lengths, with a total of 15 distinct metal–metal vectors, namely two Au–Au, seven Au–Ru and six Ru–Ru (Table 4). The two Au–Au bonds are identical within experimental error [av. 2.837(1) Å], and are similar to one of those found in $Ru_3CoAu_3(CO)_{12}(PPh_3)_3$ [11]; however, Au–Au separations in the cluster complexes mentioned in the Introduction vary between quite wide limits, values of 2.784(1) (the second Au–Au bond in $Ru_3CoAu_3(CO)_{12}(PPh_3)_3$ [11]), 2.793(4) (in $H_2Os_4Au_2(CO)_{12}(PPh_3)_2$ [4]), 2.930(1) and 3.010(1) Å (in $Ru_3Au_3[\mu_3\text{-}C(OMe)]$-

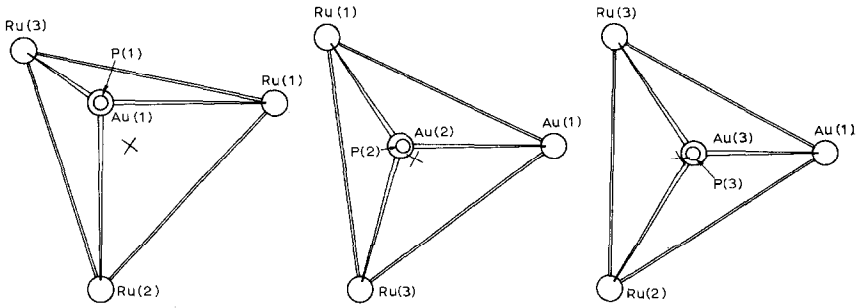

Fig. 4. Views of triangular faces in III capped by $Au(PPh_3)$ units, looking down the P–Au vector. X indicates the centroid of each face.

$(CO)_9(PPh_3)_3$ [10]) also being reported. In $VAu_3(CO)_5(PPh_3)_3$, which contains a triangular $Au_3(PPh_3)_3$ moiety capped by the $V(CO)_5$ group, the Au–Au separations are 2.768, 2.828 and 2.855 Å [14].

The three Ru–Ru bonds from Ru(4) are similar to the non-bridged bonds found in $H_4Ru_4(CO)_{12}$ [2.786(1) Å] [21], with two at 2.809 Å (av.) and one somewhat longer at 2.836(3) Å; the H-bridged bonds in $H_4Ru_4(CO)_{12}$ are 2.950(1) Å. This lengthening, together with the disposition of CO groups, suggests that the hydride may bridge this bond. The three Ru–Ru bonds in the capped face of the Ru_4 tetrahedron are considerably longer than normally found in Ru cluster carbonyl derivatives; the cause of the slight asymmetry is not obvious [two at 2.973 Å (av.), one at 3.004 Å].

The three gold atoms are arranged asymmetrically, such that Au(1) is 2.838 Å away from Ru(3), but 2.972 and 3.007 Å from Ru(1) and Ru(2), respectively. The two "outer" gold atoms cap the two $AuRu_2$ faces almost symmetrically, with Au–Ru separations of 2.821–2.850 Å (av. 2.837 Å). This asymmetry probably results from the crowded ligand environment, the PPh_3 ligands attached to Au(2) and Au(3) pushing the one on Au(1) over the Ru(1)–Ru(2) bond. This has the effect of pointing the other lobe of the *sp* hybrid towards Ru(3), with which it interacts more strongly. It is instructive to view each of the Au-capped faces along the respective P–Au vectors (Fig. 4). Both Au(2) and Au(3) are above the midpoints of the triangular faces, but Au(1) is considerably closer to Ru(3).

The core geometry found for III is the second example of a bicapped trigonal bipyramid, the first being the closely related complex $Au_3CoRu_3(CO)_{12}(PPh_3)_3$ [11]; most 7-atom clusters have structures based on monocapped octahedral metal skeletons [22]. Electron counting shows III to be a 96-electron cluster which translates using Wade's rules into a 7-atom/6-electron-pair species for which the observed bicapped trigonal bipyramid is expected [23]. Alternatively, the 96 electrons correspond to 48 cluster valence molecular orbitals [22,24] which is one fewer than the expected $(6N_{metal} + 7)$ for a compact closest-packed cluster. This is related to the condensed arrangement of metal atoms in III, although comparisons are not completely valid since the cluster valence molecular orbital calculations are strictly applicable only to clusters containing transition-metal atoms, whereas almost certainly the *d* orbitals of the gold atoms are not involved in cluster bonding *. Lauher

* If Au is considered to be an s^1 Main Group element, the electron count for the cluster is 66; again this reduces to a 7-atom/6-electron-pair system.

has predicted stability for formally electron-deficient clusters containing Group Ib metals [22].

There have been a number of discussions relating the chemistry of discrete clusters to fragments of bulk metal [25–27]. Hoare and Pal [26] have calculated the optimum geometry for bare *n*-atom fragments of metals and found that "polytetrahedral" configurations involving packing of tetrahedra face-to-face give energy minima, although other geometries based on close-packed lattice fragments often have similar stability. For 7-atom fragments the most stable geometry is the slightly distorted pentagonal bipyramid, followed successively by the monocapped octahedral and the tricapped tetrahedral arrangements which are 3.5 and 5.5% higher in energy respectively. The relevance of these calculations to molecular clusters is limited since they ignore interactions between the ligands; however, they show that there is no reason based on packing arguments for the observed geometry found for III. The rationalisation lies in the bonding preferences of $Au(PR_3)$ moieties. Calculations performed by Evans and Mingos [28] show that this fragment superficially resembles H as a ligand in that it presents one *sp* hydrid orbital suitable for cluster bonding. However, it also possesses a higher energy pair of *p* orbitals which play an important secondary role. The conclusions are that $Au(PR_3)$ fragments are best stabilised in closed triangular arrays generating tetrahedra (such as those found for III) where interactions involving the *p* orbitals of adjacent Au atoms contribute significantly to the bonding. That this model is reasonable for III is supported by the observation that two P–Au vectors point approximately to the centres of the triangular faces that they cap, while the third points to a position closer to one of the rutheniums as a result of ligand interactions (Fig. 4).

It is of interest to compare the arrangement of metal atoms found in III with those found in the related complexes $Ru_3CoAu_3(CO)_{12}(PPh_3)_3$ and $Ru_3Au_3[\mu_3\text{-}C(OMe)](CO)_9(PPh_3)_3$ (Table 3). All three clusters exhibit the same structural characteristics of an asymmetric interaction of the central gold atom with the Ru_3 or Ru_2Co face, and symmetric interactions of the outer golds with the Ru_2Au or RuCoAu faces; in addition, the Ru_4Au_3 and Ru_3CoAu_3 clusters show a dramatic increase in the Ru–Ru or Ru–Co separations in the capped face, compared with the values found in the corresponding hydrido clusters.

The observed geometries of these gold-containing mixed-metal clusters can be rationalised as follows. The first $Au(PR_3)$ group occupies a position analogous to that occupied by H in the corresponding cluster hydride. This may be either edge-bridging or face-capping, and it is in this case that the isolobal relationship between the H and $Au(PR_3)$ groups is important. However, the second and subsequent $Au(PR_3)$ groups occupy face-capping sites which develop the maximum number of tetrahedral units with Au–Au edges. This results from the necessity to maximise the interactions between *p* orbitals of neighbouring gold atoms, which thus play a steric role in developing the geometry of the resulting poly-gold clusters. These interactions are relatively weak, as shown by the wide range of observed Au–Au separations, and also by the ability of the Au_n fragment to accommodate steric interactions between peripheral ligands. We have previously described the flexibility of the Fe_3Au butterfly in $Fe_3Au(\mu_3\text{-}HCNBu^t)(CO)_9(PPh_3)$ [29]; this ready deformability of poly-gold clusters may facilitate the construction of metal atom aggregates with unusual geometries and solution dynamics.

Acknowledgements

We thank the Australian Research Grants Commission for financial support, Dr. M.R. Snow for the use of X-ray facilities and the University of Waikato, Hamilton (New Zealand), for Study Leave (BKN).

References

1 J. Lewis and B.F.G. Johnson, Pure and Applied Chem., 54 (1982) 97.
2 J.W. Lauher and K. Wald, J. Am. Chem. Soc., 103 (1981) 7648.
3 B.F.G. Johnson, D.A. Kaner, J. Lewis, P.R. Raithby and M.J. Taylor, J. Chem. Soc., Chem. Commun., (1982) 314.
4 B.F.G. Johnson, D.A. Kaner, J. Lewis, P.R. Raithby and M.J. Taylor, Polyhedron, 1 (1982) 105.
5 B.F.G. Johnson, D.A. Kaner, J. Lewis, P.R. Raithby and M.J. Rosales, J. Organomet. Chem., 231 (1982) C59.
6 P. Braunstein, J. Rose, Y. Dusausoy and J.-P. Mangeot, C.R. Acad. Sci., Paris, 294 (1982) 967.
7 B.F.G. Johnson, D.A. Kaner, J. Lewis and P.R. Raithby, J. Organomet. Chem., 215 (1981) C33.
8 M.J. Mays, P.R. Raithby, P.L. Taylor and K. Henrick, J. Organomet. Chem., 224 (1982) C45.
9 B.F.G. Johnson, D.A. Kaner, J. Lewis and P.R. Raithby, J. Chem. Soc., Chem. Commun., (1981) 753.
10 L.W. Bateman, M. Green, J.A.K. Howard, K.A. Mead, R.M. Mills, I.D. Salter, F.G.A. Stone and P. Woodward, J. Chem. Soc., Chem. Commun., (1982) 773.
11 M.I. Bruce and B.K. Nicholson, J. Chem. Soc., Chem. Commun., (1982) 1141.
12 P. Braunstein, G. Predieri, A. Tiripicchio and E. Sappa, Inorg. Chim. Acta, 63 (1982) 113.
13 J.E. Ellis and R.A. Faltynek, J. Am. Chem. Soc., 99 (1977) 1801.
14 J.E. Ellis, J. Am. Chem. Soc., 103 (1981) 6106.
15 S.A.R. Knox, J.W. Koepke, M.A. Andrews and H.D. Kaesz, J. Am. Chem. Soc., 97 (1975) 3942.
16 A.N. Nesmeyanov, E.G. Perevalova, Y.T. Struchkov, M.Y. Antipin, K.I. Grandberg and V.P. Dyadchenko, J. Organomet. Chem., 201 (1980) 343.
17 J.W. Koepke, J.R. Johnson, S.A.R. Knox and H.D. Kaesz, J. Am. Chem. Soc., 97 (1975) 3947; K.E. Inkrott and S.G. Shore, Inorg. Chem., 18 (1979) 2817.
18 SUSCAD-Data reduction programme for the CAD-4 diffractometer, University of Sydney, 1976.
19 ABSORB-Programme for correcting for absorption effects, University of Sydney, 1976.
20 SHELX 76-Programme for Crystal Structure Determination, G. Sheldrick, University of Cambridge, 1976.
21 R.D. Wilson, S.M. Wu, R.A. Love and R. Bau, Inorg. Chem., 17 (1978) 1271.
22 J. Lauher, J. Am. Chem. Soc., 100 (1978) 5305; J. Am. Chem. Soc., 101 (1979) 2604.
23 K. Wade, Adv. Inorg. Chem. Radiochem., 18 (1976) 1.
24 G. Ciani and A. Sironi, J. Organomet. Chem., 197 (1980) 233.
25 S.C. Davis and K.J. Klabunde, Chem. Rev., 82 (1982) 153.
26 M.R. Hoare and P. Pal, Adv. Phys., 20 (1970) 161.
27 J.M. Bassett and R. Ugo in R. Ugo (Ed.), Aspects of Homogeneous Catalysis, D. Reidel, Dordrecht, Holland, Vol. 3, p. 137.
28 D.G. Evans and D.M.P. Mingos, J. Organomet. Chem., 232 (1982) 171.
29 M.I. Bruce and B.K. Nicholson, J. Organomet. Chem., 250 (1983) 627.
30 M.I. Bruce, J.M. Guss, R. Mason, B.W. Skelton and A.H. White, J. Organomet. Chem., 251 (1983) 261.